

# We are IntechOpen, the world's leading publisher of Open Access books Built by scientists, for scientists

**4,800**

Open access books available

**122,000**

International authors and editors

**135M**

Downloads

Our authors are among the

**154**

Countries delivered to

**TOP 1%**

most cited scientists

**12.2%**

Contributors from top 500 universities



**WEB OF SCIENCE™**

Selection of our books indexed in the Book Citation Index  
in Web of Science™ Core Collection (BKCI)

Interested in publishing with us?  
Contact [book.department@intechopen.com](mailto:book.department@intechopen.com)

Numbers displayed above are based on latest data collected.

For more information visit [www.intechopen.com](http://www.intechopen.com)



# Fracture Toughness of Metal Castings

M. Srinivasan and S. Seetharamu

Additional information is available at the end of the chapter

<http://dx.doi.org/10.5772/50297>

## 1. Introduction

From the continuum mechanics point of view, fracture toughness of a material may be defined as the critical value of the stress intensity factor, the latter depending on a combination of the stress at the crack tip and the crack size resulting in a critical value.

The local stress  $\sigma_{local}$ , shown in Figure 1, scales as  $\sigma\sqrt{(\pi c)}$  for a given value of  $r$ , where  $\sigma$  is the remotely applied stress,  $\sigma_{local}$  is the stress in the vicinity of the crack at a distance  $r$  from the tip and  $c$  is the crack length; this combination is called the Stress Intensity Factor (K). For the type of load shown (tensile load) K is denoted as  $K_I$ . Thus,

$$K_I = Y\sigma\sqrt{(\pi c)} \quad (1)$$

where  $Y$  is a dimensionless constant to account for the crack geometry.  $K_I$  has units of MPa  $m^{1/2}$ . The material fractures in a brittle manner when  $K_I$  reaches a critical value, denoted by  $K_{IC}$ ; if there is significant crack tip plasticity, instability occurs at this critical value, leading to fracture. A simpler view of the fracture toughness is that it is a measure of the resistance of the material to separate under load when a near-atomistically sharp crack is present.

The stress intensity factors are usually identified by the subscript I for "opening mode", II for "shear mode" and III for "tearing mode". The opening mode is the one that has been investigated widely and hereafter only  $K_I$  will be considered.

Under load, a metallic material first undergoes elastic deformation and plastically deforms when its yield stress is exceeded. Fracture occurs when the ability to plastically deform under load is exhausted. The chief cause of the plastic deformation is the movement of dislocations and the resistance to its movement causes increased plastic flow stress and abatement of fracture.

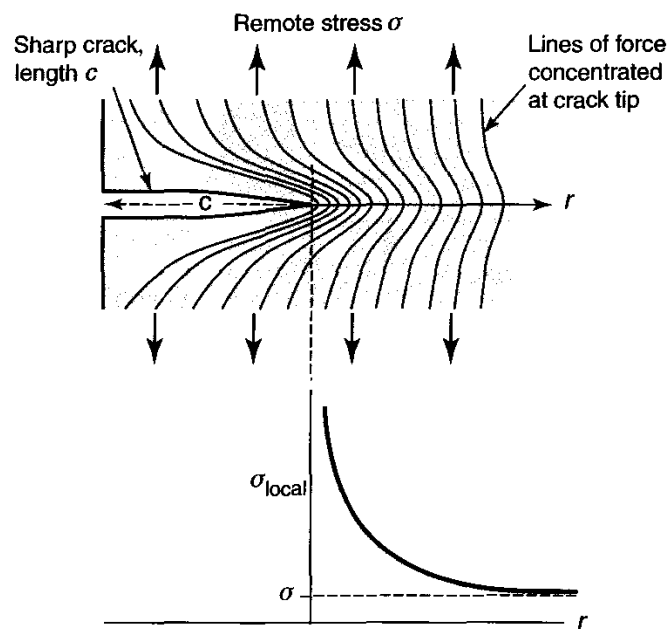


**Figure 1.** Lines of force and local stress variation from a body with sharp crack. Source: M.F. Ashby, et al [1]

The term "metal casting" represents an umbrella consisting of many variants, as will be briefly described later. The composition of the metal (alloy) will usually depend on the variant. The common factor among the variants is that they are all products of liquid-to-solid transformation, usually termed "solidification". Solidification of castings involves nucleation and growth of solid. Casting alloys usually consist of more than one phase. The simplest solidification occurs in a pure metal or an isomorphous system wherein the solid consists of only one phase. As the complexity increases, an eutectic system consisting of two solid phases may be formed, which may be totally different in properties. In low carbon steel castings, a high temperature reaction known as peritectic reaction will occur, which have some influence on the room temperature microstructure. Adding to this complexity, solid-to-solid transformations may occur, as for example, the eutectoid reaction in cast iron and steel. The phase diagrams will at best give useful guidance on the development of microstructure as they are based on equilibrium, but most castings solidify under nonequilibrium conditions resulting in departures from the phase diagram predictions. Commercial castings invariably contain various impurities that may affect the microstructure. Certain aspects of the casting microstructure have a fundamental influence on the fracture resistance [2]. It is therefore pertinent to consider the influence of valence electrons on the fracture behavior. Covalent bonds have shared electrons and the limited mobility of the electrons impedes plastic flow resulting in brittle fracture. Though metal castings in general have metallic bonds, they may contain covalent compounds such as nitrides, carbides and others as inclusions. Silicon, an important constituent in Al-Si casting alloys also has covalent bond. Ionic bonds permit better electron mobility than covalent bonds, but may cause brittle behavior when like poles interact while slipping. Metallic bonds offer least restriction to electron mobility, but as stated earlier, only a few commercial castings are made of pure metals or isomorphous alloys. An-

other important factor that needs attention is the dislocation dynamics as affected by the casting microstructure, despite the fact that the dislocation density in castings is much lower than in cold worked materials, in the as-cast state; this difference may get less under stress in castings. Unfortunately little quantitative information is available on the significance of dislocation dynamics on fracture in castings. Some casting alloys have compositions suitable for heat treatment involving solid state transformations. The microstructure is substantially changed after heat treatment and thus, in heat treated castings, the fracture behavior will usually be different as compared to the as-cast counterparts.

From the microstructural point of view, the route to increase the fracture toughness of castings would involve conflict in increasing both the fracture toughness and the yield strength. The factors of importance are [3]: improved alloy chemistry and melting practice to remove or make innocuous impurity elements that degrade fracture toughness; development of microstructures and phase distributions to maximize fracture toughness. through proper choice of composition and process variables; microstructural refinement through solidification control.

Thus it is clear that continuum mechanics provides the theoretical basis for designing against fracture in castings, but a thorough understanding of the microstructure and its effects is essential to fine-tune the final design against fracture. As noted by Ashby [4],

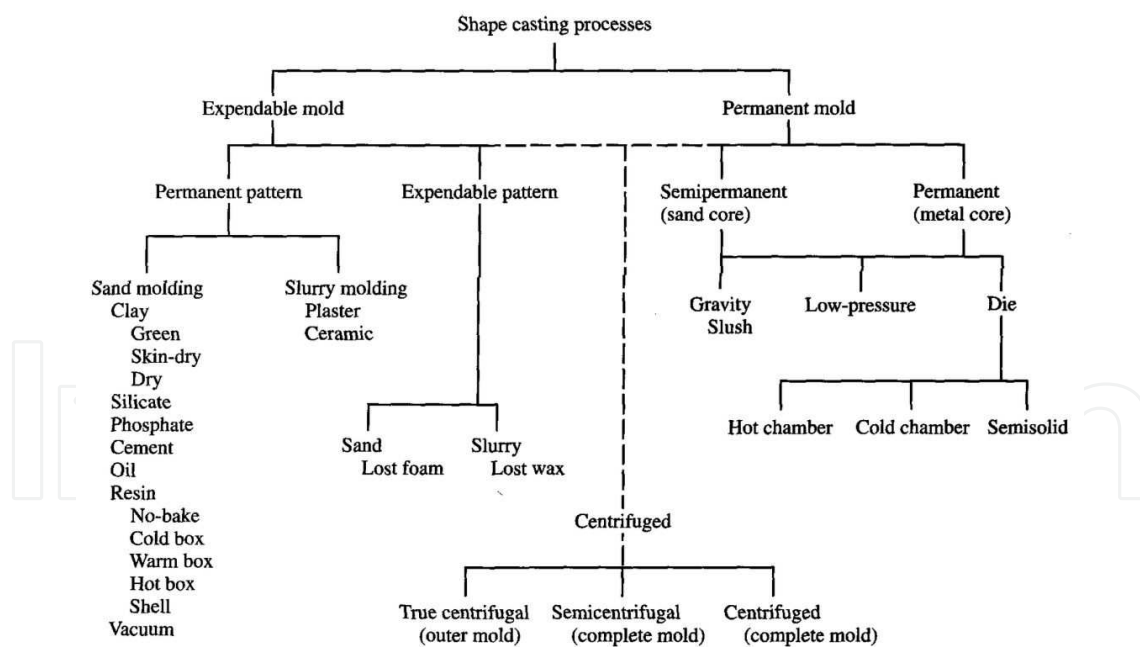


**Figure 2.** Classification of Metal Casting Processes Source: J.A. Schev, Introduction to Manufacturing Processes [6]

the real value of a well-functioning product is easy to assess, but the value of a failed product eludes evaluation until the extent of damage is known. Such knowledge can often fall under the category of "too little, too late".

In what follows, the process variables of the different members of the family of castings will be briefly considered with a view to differentiate the type of microstructure that is developed in the castings. The principles and evaluation methods of fracture toughness will then be briefly described. Selected papers from the literature will next be analyzed with a view to highlight the role of the microstructure in determining the fracture toughness of the castings. The effect of common castings defects on fracture toughness will then be very briefly considered. The use of fracture toughness - yield strength bubble charts for design against fracture [5], based on continuum mechanics, will be indicated.

## 2. Casting Processes

The umbrella covering the casting processes is shown in the figure below.

It is clear from Figure 2 that there are many avenues for making a casting, depending on the type of pattern, the type of mold and whether pressure is used for assistance in filling the mold. Not all processes are suitable for all the casting alloys. Investment casting (ceramic slurry, lost wax) is perhaps the most accommodative process for most alloys and others have limitations based on resistance to high temperature, chemical reaction and other factors. It is therefore customary to choose the casting process with due regard to the casting alloy. A recent addition to the umbrella is the squeeze casting process which is somewhat analogous to transfer molding of polymers. The microstructure of the casting is strongly affected by the process used for making it. The explanation is given below.

As stated earlier, casting is the product of solidification, which consists of nucleation and growth of solid from the liquid metal alloy). The final microstructure is decided by the composition of the alloy, the solidification rate and any melt treatment used. The alloys, based on their phase diagram may be of long-freezing range or short-freezing range type. The solidification rate is governed by the rate at which the mold is able to dissipate the latent heat and superheat of the metal poured into the mold. Permanent molds like metal and graphite molds have higher thermal conductivity than disposable molds like sand and ceramic shells and therefore provide higher solidification rates. If there is no melt treatment, finer scale microstructure can be expected when these higher conductivity molds are used. Melt treatment however, can change this picture. The object of this treatment is to refine the microstructure and the treatment is variously termed as grain refinement (in the case of single phase alloys), modification or inoculation (in the case of second phase alteration of binary alloys). The application of continuous pressure as in squeeze casting may also substantially affect the microstructure. Long-freezing range alloys cooled at a relatively slow rate, as for instance in a sand mold, tend to solidify in a "mushy" or "pasty" manner. During the progress of solidification, there will be three distinct zones: liquid, liquid+solid, solid in most cases. The liquid+solid zone is the mushy zone. If this zone has large width, the final microstructure will consist of large amount of distributed interdendritic shrinkage areas, as any feed metal from the riser will find it difficult to access many of these areas due to tortuous path involved. The width of the mushy zone is reduced as the cooling rate increases, as in metal mold castings, with consequent reduction

in distributed shrinkage. When the mushy zone is absent or too small, the solidification is termed "skin-forming" and the feed metal from a properly designed riser will have good access to the solidifying areas, thus minimizing distributed shrinkage. The shrinkage under these conditions can be totally eliminated that the feed metal has access to the final solidifying area. The application of Chvorinov's rule, which states that the solidification time is proportional to the square of the volume-to-surface area of the casting and the riser or its modifications to account for the shape, will be helpful in this regard. The basic idea is to design the riser such that its solidification is more than that of the casting and its feeding distance is appropriate to reach the last solidifying zone of the casting. In long freezing range alloys solidifying in a mushy fashion, hot tear or hot crack can develop near above the solidus temperature when the network of solid crystals is unable to sustain any thermal stress gradients, particularly when the feed metal is unable to reach these locations. These cracks are usually sharp, capable of rapid propagation. Another important consideration in castings is the porosity caused by gas liberation during solidification. Gases like hydrogen are easily soluble in the liquid state but the solubility is substantially reduced in the solid state. This may result in pores of various sizes in the solid or even microcracks when there is significant resistance to the escape of the gases. It is therefore desirable to degas the liquid metal prior to pouring in the mold. A useful law in this context is Sievert's law which states that the solubility of a dissolved gas is proportional to the square root of its partial pressure. Using this law, degassing in the liquid state can be achieved by applying vacuum (difficult and expensive) or purging with an inert gas which serves the dual purpose of lowering the partial pressure of the dissolved gas and acting as a carrier for the escape of the dissolved gas, thus reducing the harmful effect of gas porosity in the solid.

As microstructure is the key to fine-tuning of the fracture toughness of castings, the influence of casting process factors on the microstructure must be well understood, if such fine-tuning is attempted. Needless to say, metallurgical knowledge such as phase diagram and the effect of non equilibrium cooling rate on it, nucleation and growth of the different phases in the microstructure, evolution of defects through impurities and interaction of the molten metal with melting atmosphere, the furnace lining, the mold, etc., will be very useful in this regard. Heat treatment can substantially affect the microstructure and therefore, knowledge of kinetics of solid state transformations is also important to understand the effect of the particular heat treatment on the microstructure.

### **3. Basics of fracture toughness testing**

#### **3.1. Linear Elastic Fracture Mechanics [LEFM] Approach**

Linear Elastic fracture mechanics approach may be defined as a method of analysis of fracture that can determine the stress required to unstable fracture in a component.[7] The following assumptions are made in applying LEFM to predict failure in components [8].

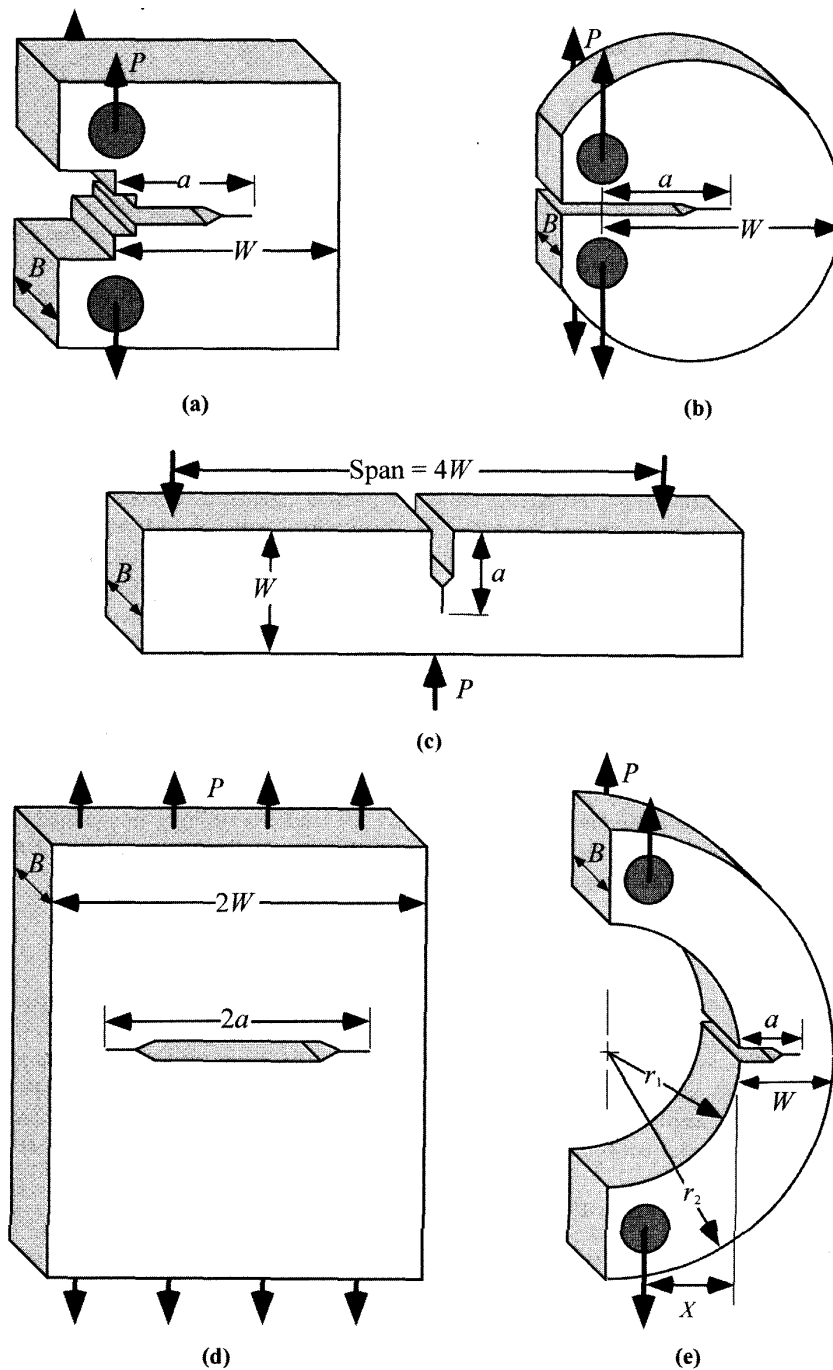


**Figure 3.** Standardized fracture mechanics test specimens: (a) compact tension (CT) specimen, (b) disk-shaped compact tension specimen, (c) single-edge-notched bend (SEB) specimen, (d) middle tension (MT) specimen and (e) arc-shaped tension specimen. Source: T.L. Anderson [9]

1. A sharp crack or flaw of similar nature already exists; the analysis deals with the propagation of the crack from the early stages.
2. The material is linearly elastic.
3. The material is isotropic.

4. The size of the plastic zone near the crack tip is small compared to the dimensions of the crack.
5. The analysis is applicable to near-tip region.

Figure 3 below shows standardized test specimens recommended for LEFM testing. Each specimen has three important characteristic dimensions: the crack length ( $a$ ), the specimen thickness ( $B$ ) and the specimen width ( $W$ ). In general,  $W=2B$  and  $a/w = 0.5$  with some exceptions. For brittle materials, a chevron-notch is milled in the crack slot to ensure that the crack runs orthogonal to the applied load.

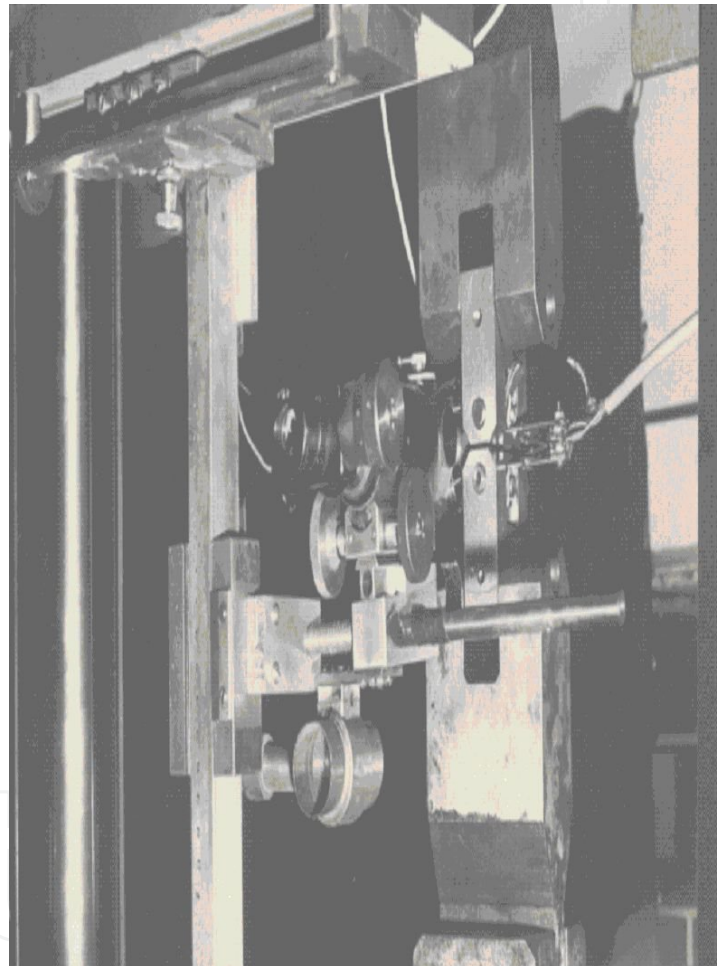


**Figure 4.** A typical view of the test set up for fracture toughness testing Source: Seetharamu [10]

In most cases fracture toughness tests are performed using either CT specimen or SEB specimen. The CT specimen is pin-loaded using special clevises. The standard span for SEB specimen is  $4W$  maximum; the span can be reduced by moving the supporting rollers symmetrically inwards.

It is to be noted that the tip of the machined notch will be too smooth to conform to an "infinitely sharp" tip. As such, it is customary to introduce a sharp crack at the tip of the ma-



chined notch. Fatigue precracking is the most efficient method of introducing a sharp crack. Care must be taken to see that the following two conditions are met by the precracking procedure: the crack-tip radius at failure must be much larger than the initial radius of the precrack and, the plastic zone produced after precracking must be small compared to the plastic zone at fracture. This is particularly necessary for metal castings as many exhibit plasticity; a notable exception is flake graphite cast iron castings made in sand molds.

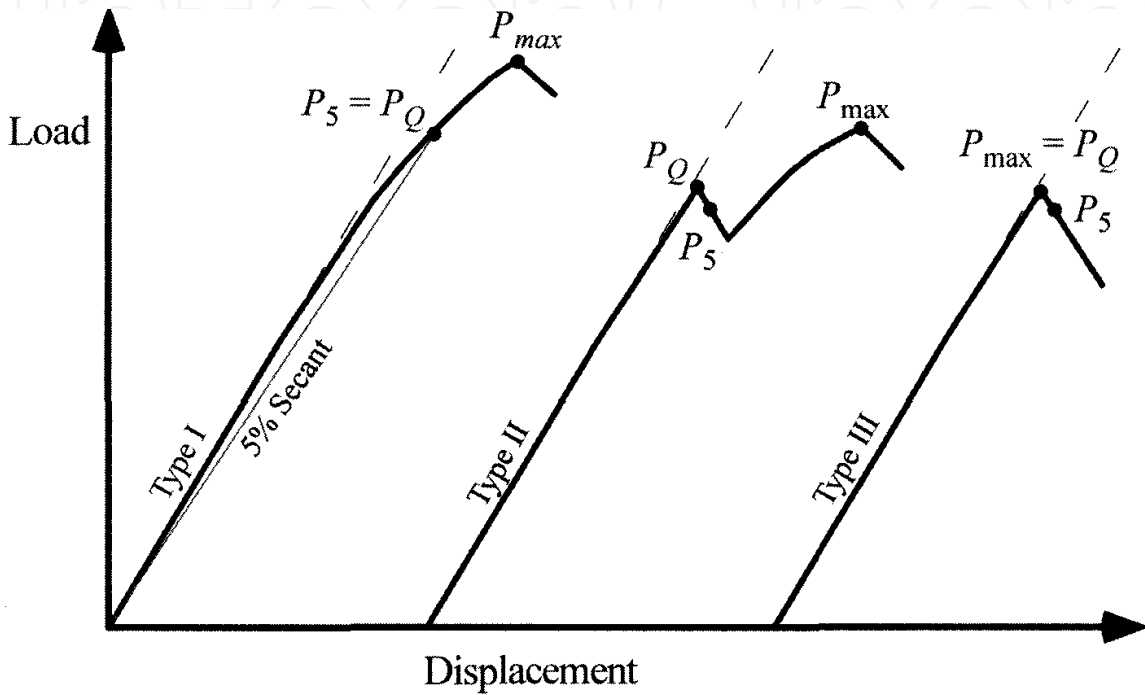


Figure 5. Type I, Type II or Type III behavior in LEFM test Source: T.L. Anderson [12]

LEFM tests are conducted as per ASTM E 399 [11]. A typical test set up is shown in Figure 4. All except the MT specimen noted in Figure are permitted to be used as per this standard. The ratio of 'a' as defined in each figure to the width W should be between 0.45 and 0.55.

The load-displacement behavior that can be obtained in a LEFM test, depending on the material, can be one of three types as shown in the Figure 5 below.

First a conditional stress intensity factor  $K_Q$  is determined from the particular curve obtained using

$$K_Q = \frac{P_Q}{B\sqrt{W}} f(a/W)$$

(2)

where  $f(a/W)$  is a dimensionless factor of  $a/w$ .

The conditional stress intensity factor  $K_Q$  is the critical stress intensity factor if

$$B, a \geq 2.5 \left( \frac{K_Q}{\sigma_{ys}} \right)^2 \quad (3)$$

where  $\sigma_{ys}$  is the yield stress of the material.

If this is not the case, the result is invalid, most likely because of significant crack tip plasticity. This would imply that triaxial state of stress required to ensure plane strain condition at the crack tip is not achieved and any determined stress intensity factor at fracture as per ASTM E399 would be an overestimate of the resistance to crack growth. Use of such values in design would be dangerous. In such cases, an elastic-plastic fracture mechanics (EPFM) method must be employed to determine the specimen's resistance to the propagation of a sharp crack.

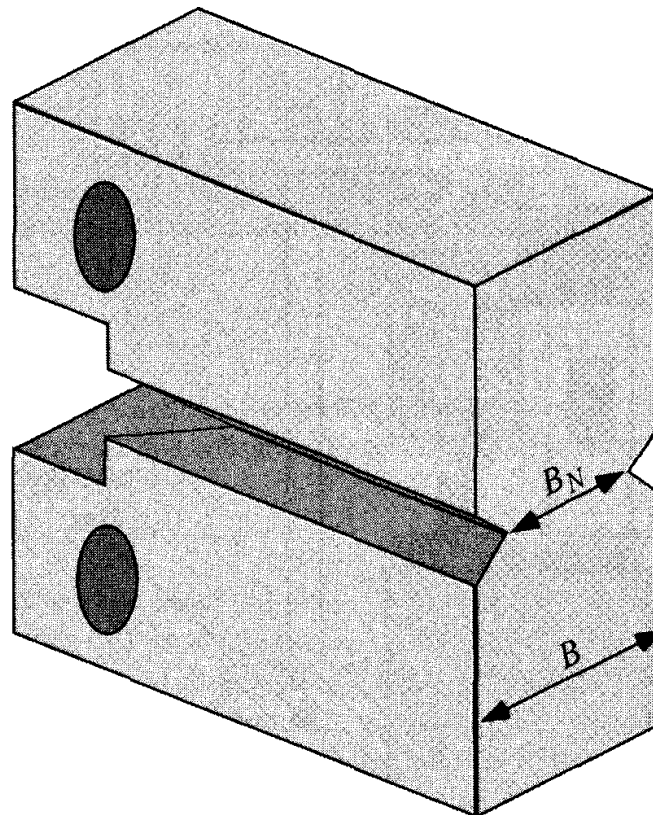


**Figure 6.** Side-grooved Fracture Toughness Test Specimen Source: T.L. Anderson [14]

### 3.2. Elastic Plastic Fracture Mechanics (EPFM) Approach

Among the different methods available to determine the sharp crack growth resistance in specimens with significant plasticity at the crack tip (much less than what is required to cause total plastic collapse) the J-integral method and the Crack-tip Opening Displacement (CTOD) have been more widely adopted. The recent trend however, is to use the J-integral

approach and only this method will be briefly described here. ASTM E 1820 [13] gives two alternative methods: the basic procedure and the resistance curve procedure. The basic procedure normally requires multiple specimens, while the resistance curve test method requires that crack growth be monitored throughout the test. The main disadvantage of this method is the additional instrumentation and skill are required. Though this method has the advantage of using a single specimen, making of multiple specimens as nearly externally identical-looking castings is not a major problem; any inconsistent results among the different specimens will give an opportunity to see if the casting microstructure is properly controlled. Therefore only the basic test procedure will be considered here.

### 3.3. The Basic Test Procedure and $J_{IC}$ Measurements

The ASTM standard that covers J-integral testing is E 1820 [13]. The first step is to generate a J resistance curve. To ensure that the crack front is straight the use of a side grooved specimen as shown in Figure 6, is recommended.

A series of nominally identical specimens are loaded to various level and then unloaded. The crack growth in each sample, which will be different is carefully marked by heat tinting or fatigue cracking after the test. The load-displacement curve for each sample is recorded. Each specimen broken open and the crack growth in each specimen is measured.

J is divided into elastic and plastic components, by using

(4)

$$J = J_{el} + J_{pl} \quad (5)$$

$$J_{el} = \frac{K^2(1-\nu^2)}{E} \quad (6)$$

$$K = \frac{P}{\sqrt{BB_N W}} f(a/W) \quad (7)$$

$$J_{pl} = \frac{\eta A_{pl}}{B_N b_0} \quad (8)$$

$\eta$  is a dimensionless quantity given by

$$\eta = 2 + 0.522(b_0/W) \quad (9)$$

In equations (6) and (7)  $b_0$  is the initial ligament length.

$A_{pl}$  is the plastic energy absorbed by the specimen determined from Figure 7.

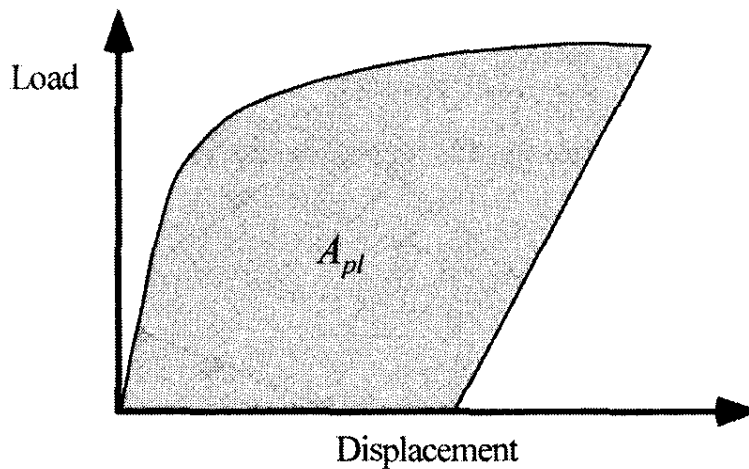


**Figure 7.** Plastic energy absorbed during J-integral test Source: T.L. Anderson [15]

The J values obtained from equation (3) are plotted against the crack extension  $\Delta a$  for each successive specimen to obtain J-R curve shown in Figure 8.

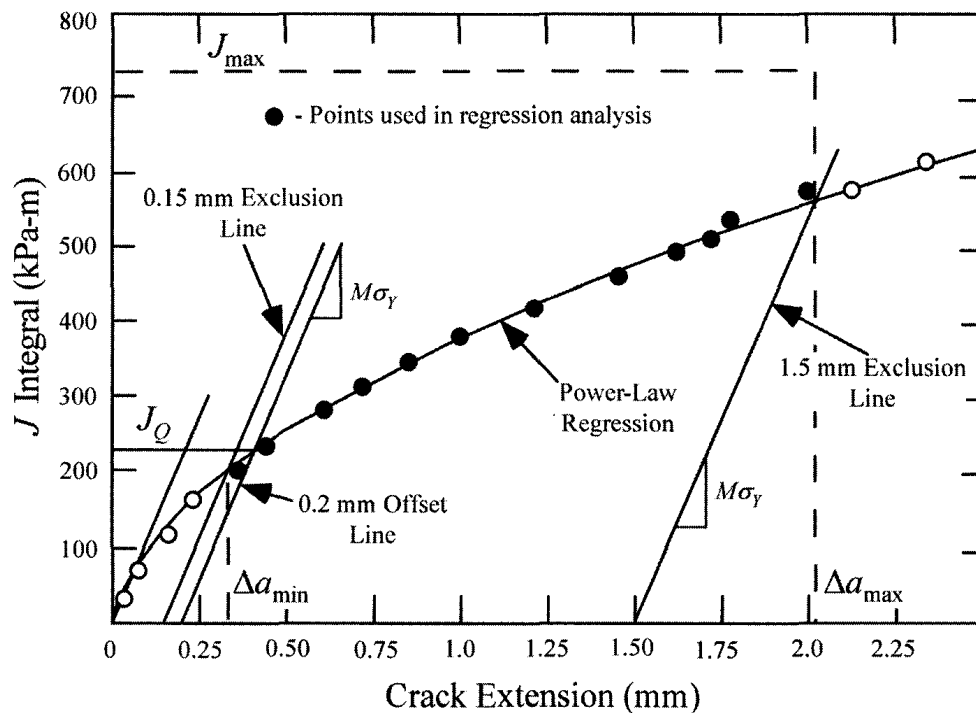


**Figure 8.** Determination of  $J_Q$  as per ASTM E 1820 Source: T.L. Anderson [16]

M value in the figure is related to crack blunting and the default value is 2. As seen in the figure, the provisional critical value  $J_Q$  is obtained from the intersection of the J-R curve with the line  $M\sigma_Y$  where  $\sigma_Y$  is the flow stress given by the average of the tensile and yield stresses.

The provisional  $J_Q$  is taken as the critical value  $J_{IC}$  if the condition:

$$B, b_0 \geq \frac{25J_Q}{\sigma_Y} \quad (10)$$

is satisfied.

The equivalence between  $J_{IC}$  and  $K_{IC}$  is given by:

$$J_{IC} = \frac{(K_{IC})^2}{E} (1 - \nu^2) \quad (11)$$

where  $E$  is the elastic modulus and  $\nu$  is the Poisson's ratio.

If it is assumed that a steel sample has a yield strength of 350 MPa, tensile strength of 450 MPa and Young's modulus ( $E$ ) of 207 GPa and fracture toughness of  $200 \text{ MPa}\sqrt{m}$ , it can be shown that E 399 thickness requirement for validity is 0.816 m, while the E 1820 thickness requirement for validity, based on the equivalence shown in equation (6) is only 11 mm. The advantage of E1820 approach over E399 approach in regard to valid specimen thickness requirement is thus obvious.

## 4. Fracture toughness of metal (alloy) castings

In what follows reported fracture values of various castings will be presented and discussed.

### 4.1. Aluminum alloy castings

In recent times, the most widely studied nonferrous casting alloys for fracture behavior are aluminum casting alloys. Among them, aluminum silicon alloys have attracted the most attention as they are widely used because of good castability and high strength-to-weight ratio. The microstructure of aluminum silicon alloys can be significantly affected by changes in the process variables as typically shown below in Figure 9 for aluminum-5% silicon alloy. The figure shows the variation of microstructure with cooling rate. Figure 9(a) refers to a sand casting where the cooling rate is the lowest among the three, sand cast, permanent mold cast and die cast. The dendrite cells are large, the silicon flakes (dark) are coarse and iron-silicon-aluminum intermetallics (light grey) are seen. The resistance to crack propagation will be the lowest with this type of microstructure. Figure 9(b) refers to a permanent mold casting where the cooling rate is higher than in a sand castings. It is seen that there is refinement in both primary aluminum and eutectic silicon as well as the intermetallics. The resistance to crack growth will be higher than in sand castings. Figure 9(c) shows the microstructure of a die casting of the alloy where high degree of refining of dendrite cells and eutectic silicon are seen. Other things being equal, the resistance to crack growth will be

maximum in this type of microstructure. However other things will not be equal in general, the main factor being the yield strength of the casting. Thus crack tip plasticity will be high in the sand casting, intermediate in the permanent mold casting and lowest in die casting. Thus the fracture toughness increase in the casting will not be in direction proportion to the reduction in cooling rate. The factors favoring increase in fracture toughness would be decreased dendritic cell size and refinement of the covalent bonded silicon and mixed bonded intermetallics. The opposing factor would be reduced plasticity due to increase in yield strength, both due to primary cell and eutectic refinement.

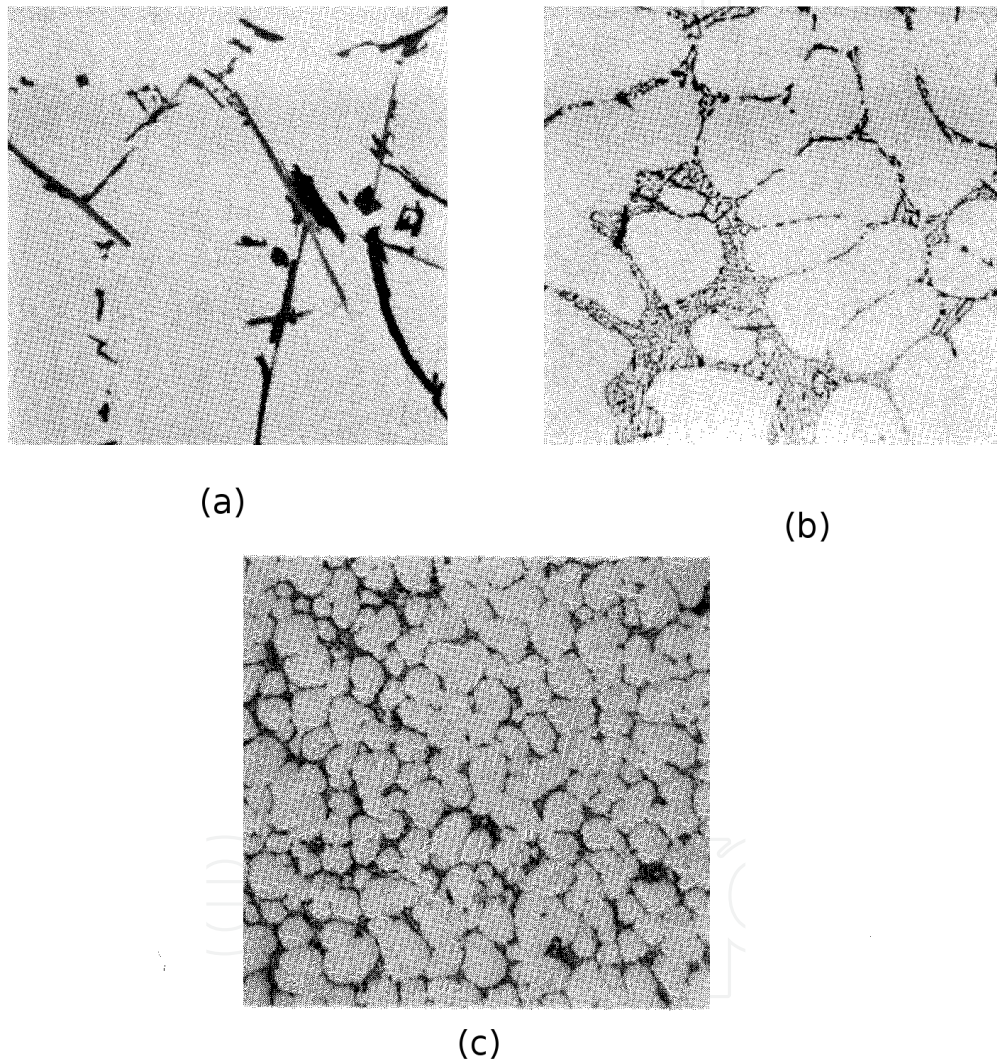


**Figure 9.** Microstructure of aluminum casting alloy 443 (Al-5%Si) (a) Alloy 443-F, as sand cast, (b) Alloy B443-F, as permanent mold cast, (c) Alloy C443-F, as die cast All were etched with 0.5% hydrofluoric acid and photographed at 500 X. Source: W.F. Smith [17]

Figure 10 refers to the microstructural variations brought by heat treating alloy 356- Al-7% Si-0.3%Mg (sand cast, constant cooling rate). Figure 10(a) refers the microstructure after artificial aging. The coarse dark platelets are silicon, black script is  $Mg_2Si$  and the light scripts

are intermetallics of iron-silicon-aluminum and iron-magnesium-silicon-iron. The dendrite cell is coarse. Figure 10(b) refers to alloy 356-F as sand cast, which is modified with 0.25% sodium. The cells are still coarse but the silicon particles are refined and in the form of interdendritic network. Figure 10(c) refers to alloy 356-T7 which is modified with 0.025% sodium, solution treated and stabilized. The microstructure shows rounded interdendritic silicon and iron-silicon-aluminum intermetallics. Here again the opposing factors discussed above will come into play but the plasticity in primary aluminum will be around the same and the dual causes for increase in yield strength as in the previous case will not be present.

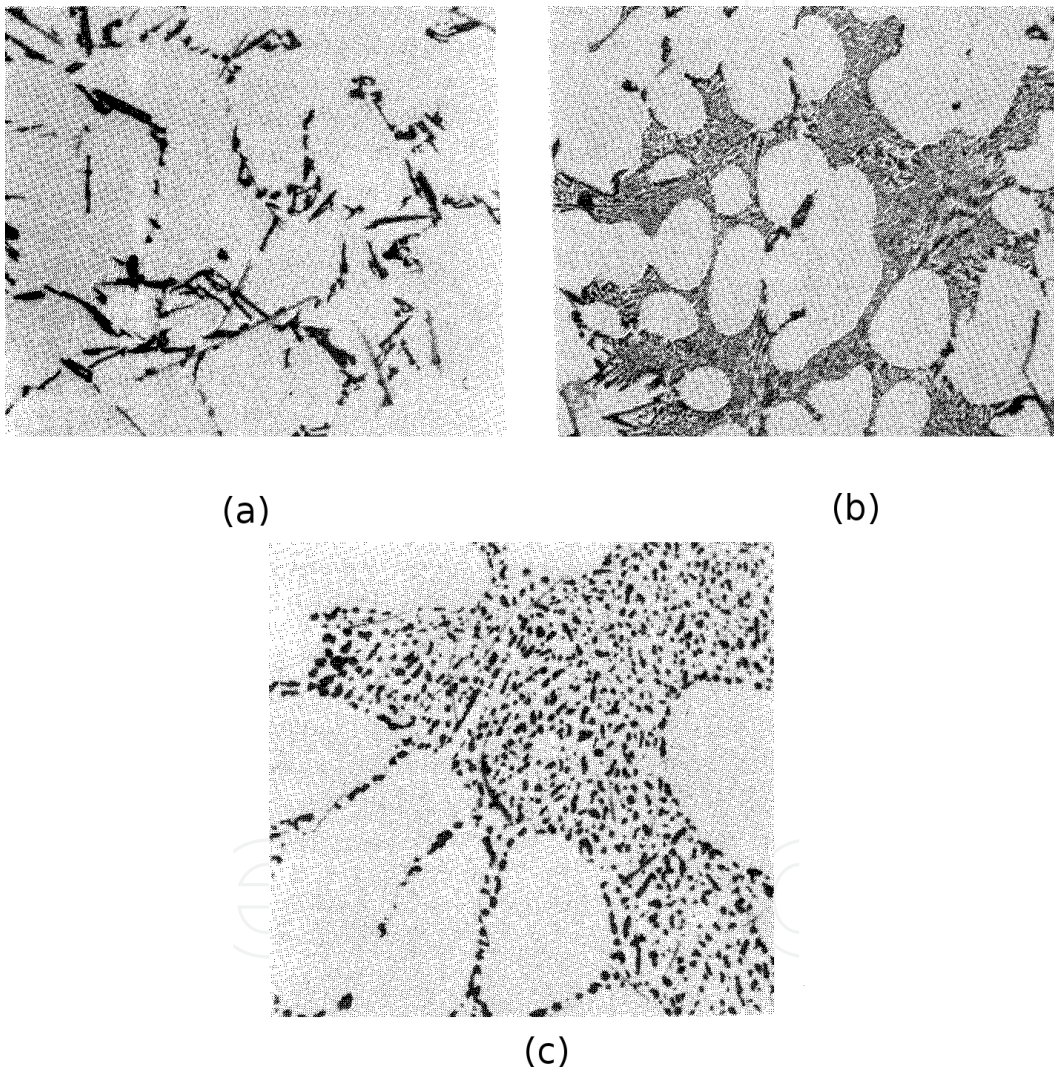


**Figure 10.** Microstructure of alloy 356 sand cast and heat-treated in different conditions (a) alloy 356-T51: sand cast, artificially aged, (b) alloy 356-F: as sand cast, modified with 0.025% sodium, (c) alloy 356 T7: sand cast, modified by sodium addition, solution treated and stabilized. All were etched with 0.5% hydrofluoric acid and photographed at 250 X. Source: W.F. Smith [18]

Having noted these factors in affecting the fracture toughness, some recent papers on fracture toughness of aluminum alloys will now be examined.

Hafiz and Kobayashi [19] studied the fracture toughness of a series of aluminum silicon eutectic alloy castings made in graphite and steel molds. The microstructure was varied by treating with different amounts of strontium. J-R curve obtained from multiple specimens was used to determine  $J_Q$  values. Extensive microstructural and SEM fractographic studies were made. They defined a ratio  $(\lambda / DE_{Si})$  where  $\lambda$  is the silicon particle spacing and  $(DE)_{Si}$  is the equivalent silicon particle diameter. They also defined the void growth parameter as  $VGP = \sigma_y (\lambda / DE)_{Si}$ . They found that the equation  $J_Q = -9.94 + 0.38(VGP)$  is obtained in their samples, with  $J_Q$  varying in a straight line fashion from about 7 kJm<sup>-2</sup> to about 78 kJm<sup>-2</sup> when the VGP varied from 50 MPa to 200 MPa. Their main conclusion is that in eutectic Al-Si alloy castings, greater the refinement of eutectic silicon, higher will be the fracture toughness.

Kumai, et al, [20] on the other hand focused on the dendrite arm spacing of alloy A356, (which is hypoeutectic) permanent mold and direct chill (semi continuous) cast tear test samples in their work. The area under the load-displacement curve was determined as the total energy and was divided into energy for initiation and propagation. It was found that in direct chill casting, both initiation and propagation energies increased with decrease in the dendrite arm spacing (DAS); decrease in DAS resulted only in increase of propagation energy in permanent mold casting. The fracture surface was perpendicular to the load in permanent mold castings while it was slanted in DC casting indicating higher energy absorption during the fracture process. This test could at best be qualitative in determining the fracture behavior.

Tirakiyoglu [21] has examined the fracture toughness potential of cast Al-7%Si-Mg alloys. He has reported that based on Speidel's data [22] a relationship of the form:

$$K_{IC}(\text{int}) = 37.50 - 0.058\sigma_{ys} \quad (12)$$

can be developed between the maximum (intrinsic) fracture toughness and yield strength of this alloy. However, as suggested by Staley [23] there are several extrinsic factors such as porosity, oxides and inclusions that tend to lower the fracture toughness. If these extrinsic factors are eliminated the intrinsic fracture toughness can be higher, given by:

$$K_{IC}(\text{int}) = 50.0 - 0.073\sigma_{ys} \quad (13)$$

Equation (11) gives the potential maximum fracture toughness of the Al-7%Si-Mg cast alloy in the absence of defects. A nice feature of this paper is the listing of dendrite arm spacing of different types of aluminum-silicon-magnesium alloy castings.

Tohgo and Oka [24] have studied the influence of coarsening treatment on fracture toughness of aluminum-silicon-magnesium alloy castings. The alloy: Al-7%Si-0.4%Mg was cast in permanent mold and solution treated for 6 hr at 803 K followed by aging for 6 hr at 433 K. One batch was tested in this condition while a second batch was further given a coarsening treatment at 808 K for 50 hr, 100 hr, 150 hr and 200 hr. J-R curves were constructed using 5 specimens and  $J_Q$  values were determined. The fracture toughness increased to 27 MPam<sup>1/2</sup> after coarsening of silicon, as compared to 20.8 MPam<sup>1/2</sup> for uncoarsened sample. The au-



thors attribute the improvement to the increased plastic deformation of  $\alpha$ -Al owing to more uniform distribution of silicon particles, energy dissipation due to damage of silicon particles around a crack and the rough fracture path in the coarsened sample.

Kwon, et al [25] have investigated the effect of microstructure on fracture toughness of rheo-cast and cast-forged A356-T6 alloy. Interdendritic silicon was observed in the microstructure of rheo-cast sample while there was alignment of cells in the cast-forged sample along with more uniform dispersion of silicon particles. Fractographs of fracture toughness specimens indicated cleavage type fracture in the rheo-cast sample while there was fibrous fracture in the cast-forged sample. As to be expected the fracture toughness of the rheo-cast sample was  $20.6 \text{ MPam}^{1/2}$  while the cast-forged sample showed a fracture toughness of  $24.6 \text{ MPam}^{1/2}$ .

Alexopoulos and Tirayakioglu [26] have determined the fracture toughness of A357 cast aluminum alloys with a few minor chemical modification. The raw stock for further machining required for studies was continuously cast with intent to keep porosity and inclusions at a minimum level. The continuous casting process is the patented SOPHIA process capable of providing cooling rates of up to  $700 \text{ K/min}$ . As compared to an investment cast sample, the dendrite arm spacing in the SOPHIA-cast sample would be lower by about 33%. The fracture toughness values, determined from CTOD measurements, ranged from about  $18 \text{ MPam}^{1/2}$  to about  $29 \text{ MPam}^{1/2}$ , depending on the composition and the heat treatment. The higher value was obtained in the plain A357 cast by SOPHIA process and subjected to solution treatment for 22 hr at  $538 \text{ C}$  and aged for 20 hr at  $155 \text{ C}$ . The main aim of these authors was to establish correlation between tensile properties and fracture toughness and the major part of the paper deals with evaluation of tensile behavior under different conditions.

Lee, et al [27] have investigated the effect of eutectic silicon particles on the fracture toughness of A356 alloy cast using three different methods: low pressure casting (LPC), casting-forging (CF) and squeeze casting (SC). They used ASTM E 399 procedure and as to be expected, got invalid fracture toughness results (sample thickness was 10 mm). They also conducted in-situ SEM studies on crack morphology, where plane stress was present. Thus only qualitative comparisons can be made on the influence of the three different casting processes on the fracture toughness. A notable observation is that significant shrinkage pores were present in LPC samples, while they disappeared in CF and SC samples, evidently due to the higher pressures applied. The eutectic cell size was the least in SC samples while it was similar in size in PC and CF samples. SEM fractographs from all the three samples showed fibrous fracture, with LPC samples showing the additional effect of stress concentration at the edges of shrinkage cavity. Though the SC sample had the most refined microstructure, the apparent fracture toughness was the lowest on account of reduced spacing between the eutectic silicon particles that apparently encouraged fracture initiation.

Tirakiyoglu and Campbell [28] have analyzed the fracture toughness of Al-Cu-Mg-Ag (A201) alloy from data on premium quality castings. When molten metal is poured into a mold, the Reynolds number is invariably in the turbulent flow region to facilitate proper filling of the mold. In aluminum alloys, the surface oxide that forms as a result becomes folded into the bulk of the melt. These oxide "bifilms" have neutral buoyancy, unlike in say, steel castings and tend to travel with the melt into the mold cavity. As they do not bond with the

liquid, the solidified casting will have the bifilms remaining as cracks due to the discontinuity. Also, the layer of air in the folded bifilms can grow into a pore or remain as a crack in the casting. The authors point out that in aluminum (and other crossing alloys) this is perhaps the most ignored defect as far as plans for elimination of defects are concerned. This extrinsic defect will result in the intrinsic fracture toughness not being attained. As per the authors, the intrinsic fracture toughness in A301 casting can be represented by:

$$K_{IC} = \left\{ \ln \left[ 1 + \frac{\exp(-0.0032\sigma_{ys})}{100} \right] \right\}^{3/2} \left( \frac{2k E' \sigma_{ys}}{3} \right)^{1/2} \quad (14)$$

Here,

$$E' = \frac{E}{1-\nu^2} \quad (15)$$

The intrinsic value of  $K_{IC}$  can exceed 45 MPa m<sup>1/2</sup> if the yield strength is around 350 MPa.

#### 4.2. Steel Castings

Jackson [29] has published a comprehensive paper on the fracture toughness of steel castings. He has considered that steel is susceptible to ductile-brittle transition and has reported the fracture toughness for lower shelf using LEFM and for the upper shelf using EPFM. While the LEFM method he used was the same as ASTM E399, use of CTOD was more in vogue in England at the time he wrote the paper and therefore either the critical CTOD ( $\delta_C$ ) or the equivalent  $J_{IC}$  have been reported in the paper, using the relation:

$$\delta_C = \frac{J_{IC}}{\sigma_{ys}} \quad (16)$$

Steel	$K_{IC}$ (MPa m <sup>1/2</sup> )	$\sigma_{ys}$ (MPa)	Critical flaw size (mm) Surface Embedded
1. 0.5%C, 1% Cr	46	480	3.7 4.4
2. 1.5%Ni-Cr-Mo	86	740	5.4 6.2
3. 1.5%Ni-Cr-Mo	104	1280	2.6 3.2

**Table 1.** Table 1. The fracture toughness, yield strength and chosen values of critical flaw size for three cases are shown in Table 1.

Steel 3 was vacuum melted while the other two were air melted, showing that a stronger steel has the disadvantage of lower critical flaw size (elliptical flaw, ratio of major-to-minor axis is 8-to-1).

One important point made by Jackson is that the chemical composition effects on fracture toughness may be masked by those of features such as shrinkage. Though it is known that increasing sulfur and phosphorus leads to decrease in fracture toughness, in the researcher's experiments, shrinkage masked this expected effect. Shrinkage encountered in the crack path may cause multiple crack fronts deviating from the main path resulting in increased fracture toughness to be observed; this overestimates the intrinsic fracture toughness and may cause problems when applied in design. The best remedy is therefore is to minimize shrinkage using proper feeding techniques.

As reported by Jackson, in the case of a 0.5%Mo, 0.33% V steel casting the lower shelf fracture toughness is about  $55 \text{ MPa m}^{1/2}$  (temperature  $< 60\text{C}$ ) while the upper shelf value increases to about  $180 \text{ MPa m}^{1/2}$  (temperature  $> 110 \text{ C}$ ). This behavior is inherent in BCC alloys like steel and should be considered in equipment where there is a wide difference between the cold start temperature and operational temperature. The problem then is to avoid brittle fracture during cold start and onset of plastic instability at normal operating temperatures.

Barnhurst and Gruzleski [30] have investigated the fracture toughness of high purity cast carbon and low alloy steels. A notable feature of this work was that only blocks that were found to be radiographically sound were used for the preparation of fracture toughness specimens. The inclusion level in all the castings were low enough to classify them as extremely clean. The steel compositions were according to AISI/SAE 1030, 1527, 1536, 2330, 2517 for low carbon steels, 1040, 5140, 1552, 5046, 2345 for medium carbon steels and 1055, 5155, 3450, 52100 for high carbon steel. Other than carbon, each grade no other element or one alloying element, with impurities being kept to a minimum. All castings were austenitized in the range of 840 C- 900 C depending on the alloy, for 4 hr, oil quenched, held mostly at 650 C for 2 hr (with two exceptions: two samples directly air cooled from 900 C soak, one sample held at 300 C after oil quenching and then air cooled). The fracture mode in most castings was ductile, with only a few showing cleavage or mixed ductile/cleavage fracture. The  $K_{IC}$  values determined from  $J_{IC}$  ranged from  $41.6 \text{ MPa m}^{1/2}$  (1.0 C, 1.61 Cr) to  $247.8 \text{ MPa m}^{1/2}$  (0.25 C, 4.60 Ni). The conclusions drawn were that under carefully controlled composition, heat treatment, inclusion and impurity content, exceptional fracture toughness values at room temperature can be obtained, at the expense of tensile properties. The critical flaw sizes would exceed the section thickness of most designs. Under normal production conditions where attainment of such high purity is impractical, this study does provide the guidelines that the influence of alloying elements like nickel, chromium and manganese is relatively small at medium carbon levels and that heat treatment, additions of molybdenum and silicon may have significant influence on room temperature fracture toughness.

Chen, et al [31] have studied random fracture toughness values of China Railway Grade B cast steel wheels using LEFM approach. The wheel was first stress relieved, and then the rim was quenched and tempered, while the hub was shot peened.  $K_Q$  values reported range from  $50.52 \text{ MPa m}^{1/2}$  to  $63.77 \text{ MPa m}^{1/2}$  in the wheel hub and,  $60.70 \text{ MPa m}^{1/2}$  to  $76.40 \text{ MPa}$

$m^{1/2}$  in the wheel rim. Only the specimen thickness (~25 mm) has been indicated but the yield strength values have not been provided: it is therefore difficult to say whether these values are valid or not. Narrative description of the fracture surface using SEM indicates the predominance of cleavage with little evidence of fibrous rupture.

Kim, et al, [32] have evaluated the fracture toughness of centrifugally cast high speed steel rolls. The carbon equivalent, defined as  $C + 1/3 Si$  was in the range of 1.89 to 2.28 and the tungsten equivalent, defined as  $W + 2 Mo$  was in the range of 9.82 to 13.34. Vanadium content was varied between 3.95 and 6.26 and the chromium content was kept constant in the range of 4.0-6.0. Precracking presented difficulties and therefore the authors used 30-50  $\mu m$  machined notch. Tests were made otherwise as per ASTM 399.  $K_{IC}$  values were in the range of 21.4 MPa  $m^{1/2}$  to 28.2 MPa  $m^{1/2}$ . They have concluded that the fracture toughness is determined by the total fraction of carbides, characteristics of the tempered martensitic matrix, distribution and fraction of intercellular carbides and fraction of cleavage and fibrous mode on the fracture surface. The best fracture toughness was obtained when a small amount of intercellular carbides was distributed in a relatively ductile matrix of lath martensite.

James and Mills [33] have investigated the fracture toughness of two popular as cast stainless steels, CF8 and CF8M. Toughness tests were conducted at 24 C, 371 C, 427 C and 482 C using multiple specimen J-R curve method. Exceptionally high  $J_{IC}$  values, in the range of 1397 kJ/m<sup>2</sup> at 24 C to 416 kJ/m<sup>2</sup> at 482 C demonstrated that fracture control is not a concern in unirradiated condition. However, neutron irradiation reduces  $J_{IC}$  by an order of magnitude and therefore fracture control becomes essential.

### 4.3. Cast Iron

The metallurgy of cast iron is among the most complex of all alloys. Cast iron shows metastability anomaly. Under certain conditions of composition and cooling rate the eutectic formed upon solidification consists of austenite and graphite. Under certain other conditions an eutectic of austenite and iron carbide is formed. The former is known as graphitic cast iron, while the latter as white cast iron. In low sulfur and oxygen cast iron melts, if magnesium is added so that its residual amount is 0.05% or above (but not too high) the graphite formed will be nodular rather than the flake form found in untreated graphitic cast iron melts. In the latter the flake may be of undercooled type (Type D- when the sulfur content is low in sand or investment castings or with normal sulfur when the cooling rate corresponds to that in permanent molds); it will be in the interdendritic form, with branching). Under normal conditions found in commercial sand castings, the graphite will be a part of the eutectic cell formed with austenite, graphite having a loose "cabbage" shape with the interleaf region occupied by eutectic austenite. Adding a silicon-bearing inoculant will increase the number of eutectic cells in flake cast iron and nodule count in nodular (or, ductile) iron. The white cast iron forms graphite in the solid state when heat treated (and is called malleable iron), but the melt-formed graphite in the other two types of cast iron will be largely unaffected by any solid state transformation. In recent times another type called compacted graphite cast iron has been developed where the residual magnesium is lower than in ductile iron. All types of cast iron noted above are governed by eutectoid decomposition, which

means that the matrix may consist of various combinations of ferrite and pearlite under near-equilibrium conditions. These irons are also affected by isothermal or continuous cooling transformations at nonequilibrium rates giving rise to bainitic or martensitic or tempered martensitic cast irons. In recent times, a bainitic ductile iron known as austempered ductile iron (ADI) has become popular in industrial applications. In what follows, investigations on the fracture toughness of some of these cast irons will be briefly discussed.

The exact reasons for the formation of different types of graphite in cast iron have been a matter of debate for many years. The type of graphite found in commercial cast irons may have one or more of the following types: flake (Type A), undercooled (Type D), coral, compacted, nodular. A generalized view, based on the growth of graphite (in the liquid state) is presented in Figure 11 below.

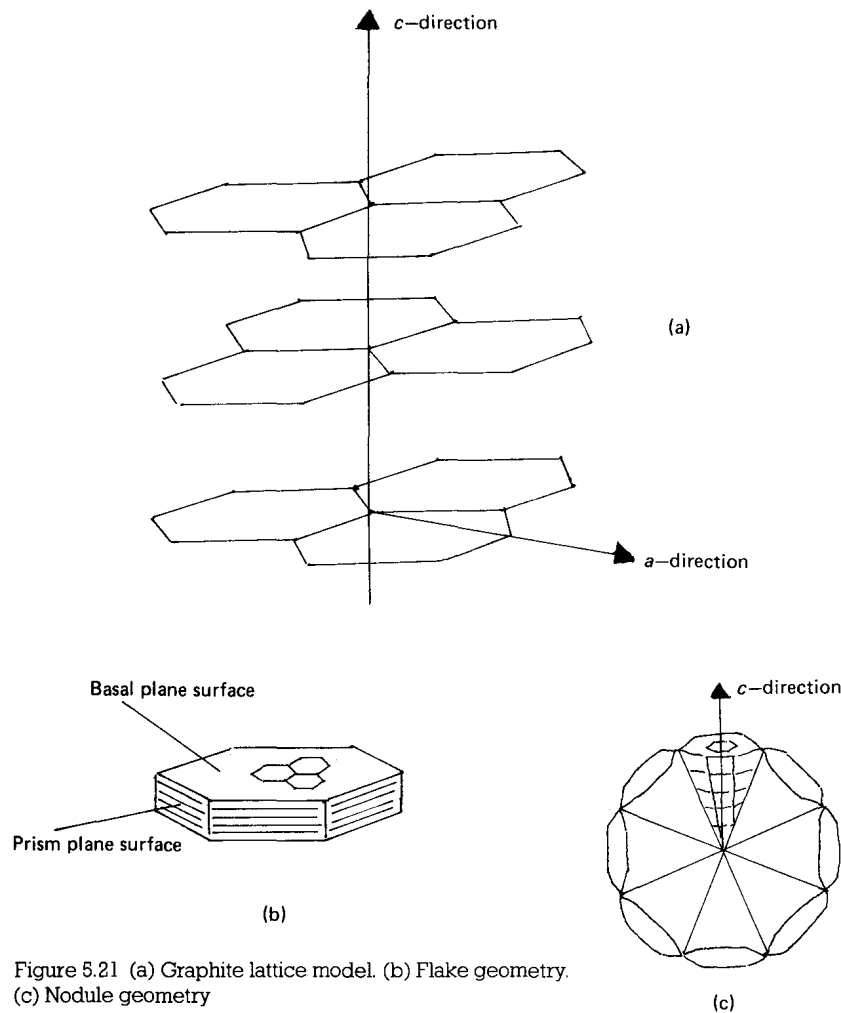


Figure 5.21 (a) Graphite lattice model. (b) Flake geometry. (c) Nodule geometry

Figure 11. Extremities in the growth of graphite in the liquid Source: Elliott [34]

Graphite has a layered hexagonal lattice structure (a), with strong covalent bonds in the hexagonal chains, with the layers bonded by weak secondary bonds. The hexagonal plane is called the basal plane and the edge of the block formed by bonding of layers with weak

bonds is called the prism plane. The basal planes tend to grow in the "a" direction and the prism planes in the "c" direction. When growth in the "a" direction is dominant, flake form is obtained, the thickness being determined by the growth rate and the graphite source; slower the growth rate and lower the number of eutectic cells, the thicker would be the flake. When "a" growth is suppressed and "c" growth is fully encouraged, nodular form results. Intermediate forms like Type D, coral or vermicular forms result when there is progressive resistance to the formation of Type A, or alternatively, decreasing encouragement to the nodular shape formation. It is to be realized that the exact reasons for these resistances or discouragements may be due to the interaction of fine-scale multiple activities, often at the atomic scale, related to both nucleation and growth. Thus, at this time one has to accept that these different forms of graphite, which curiously are relatively stable forms during the life of a component, do exist and there is need to understand, for instance, the details of how the crack propagation is affected by their interactions with the fine-scale features of the neighborhood of the crack..

The fracture toughness of graphitic cast iron is determined by the type of graphite, the type of matrix and the interaction between the graphite and the matrix. In view of numerous combinations possible, the fracture toughness could be expected to vary over a wide range: this is indeed the case. Once again it follows that to fine-tune the fracture toughness of cast iron the microstructural features should be analyzed and examined if corrective measures can be taken, consistent with cost-benefit analysis.

The fracture toughness of flake cast iron ranges from 11-19 MPa m<sup>1/2</sup> [35]. Whether these are valid results as per ASTM E399 is subject to the acceptance of the tensile strength instead of the yield strength for validity criterion, as flake cast iron has non linear elastic part in the stress-strain curve and 0.2% offset method can not be applied to determine the yield strength. Thus the above noted values may be cited by some as K<sub>Q</sub> and by others as K<sub>IC</sub>. In critical applications these low value force the assumption of a high factor of safety. A pertinent observation with respect to flake cast iron is that the ductile-brittle transition temperature is well above the room temperature and therefore the fracture toughness at normal or below-normal operating temperatures seems to be unaffected by the temperature.

Because of the steel-like mechanical behavior of nodular graphite cast iron, the fracture toughness of this iron has been vastly studied. The fracture toughness values range from about 25 MPa m<sup>1/2</sup> in an iron with yield strength of about 450 MPa to nearly 60 MPa m<sup>1/2</sup> in an iron of yield strength of 370 MPa [36]. It is possible that the intrinsic fracture toughness of nodular iron would be higher if the inherent shrinkage, among the highest in cast irons, is reduced. A particular grade, D7003 (quenched and tempered) poses both good fracture toughness and high yield strength. Salzbrenner [37] evaluated the fracture toughness of samples of different compositions, but adopted a constant heat treatment with intent to have a ferritic matrix. The heat treatment involved solutionizing at 900 C for 4 hr, followed by slow furnace cool (at 10 C/hr) to 700 C and holding at this temperature for 24 hr followed by slow cooling. He followed EPFM approach and obtained fracture toughness values ranging from a high of 79 MPa m<sup>1/2</sup> (with small, well distributed nodules) to as low as 25 MPa m<sup>1/2</sup> in a sample with non-spherical nodules. The better fracture toughness of nodular iron in rela-

tion to flake cast iron is often attributed to the relatively smooth graphite-matrix interface in the former. This statement may however, be an oversimplification as there are factors such as the diversion of the crack and ability to absorb energy in the interlayer regions of the nodule to be considered.

Doong, et al [38] have investigated the influence of pearlite fraction on fracture toughness of nodular iron and their results show that when the pearlite fraction is 4% or 27% the fracture toughness shows a decreasing trend in the range of -75 C to 75 C, while the fracture toughness of samples with 67% and 97% pearlite show an increasing trend in the same temperature range. The nodularity in all these castings was 95% or better..

Nodular iron castings are generally made in sand molds but the present authors investigated the fracture toughness of permanent mold-cast magnesium-treated iron. A hypereutectic composition with a high silicon percentage (3-3.4%) was used to avoid the formation of iron carbide in the as-cast state. The graphite consisted of overlapping nodules, possibly as a result of high thermal convection in permanent molds. It is also possible that inoculation was needed to provide more nucleation of graphite and reduce the possibility of overlapping, by rapid austenitic shell formation around the nodules.

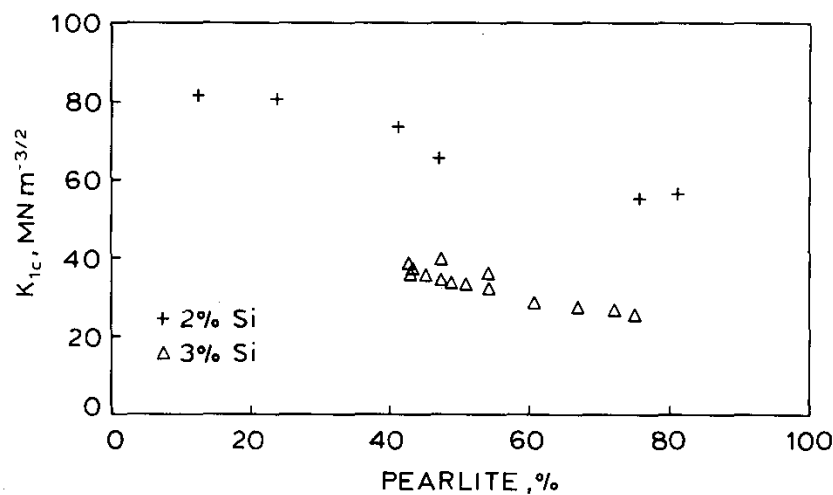


**Figure 12.** Effect of pearlite content on fracture toughness of permanent mold ductile iron Source: Bradley and Srinivasan [39]

Figure 12 seen above shows the effect of pearlite content in two types of permanent mold ductile iron. The top curve refers to a melt with 2% silicon, which led to a chilled casting and was soaked at 900 C and cooled at different rates to obtain different combinations of ferrite and pearlite in the matrix. The lower curve refers to a set of chill-free castings, obtained by solidifying castings with 3% silicon. Different pearlite/ferrite combinations were produced by varying the casting thickness. It is seen that increase in silicon significantly lowers the fracture toughness. A possible reason is that on increasing the silicon level to 3%, the ductile-brittle transition temperature is raised to well above the room temperature. It is also pos-

sible that any residual stress present in the as-cast state is minimized in the heat treated state. In any case the differences in the modes of fracture in the two cases are clearly seen in Figure. 13 and Figure 14 shown below.

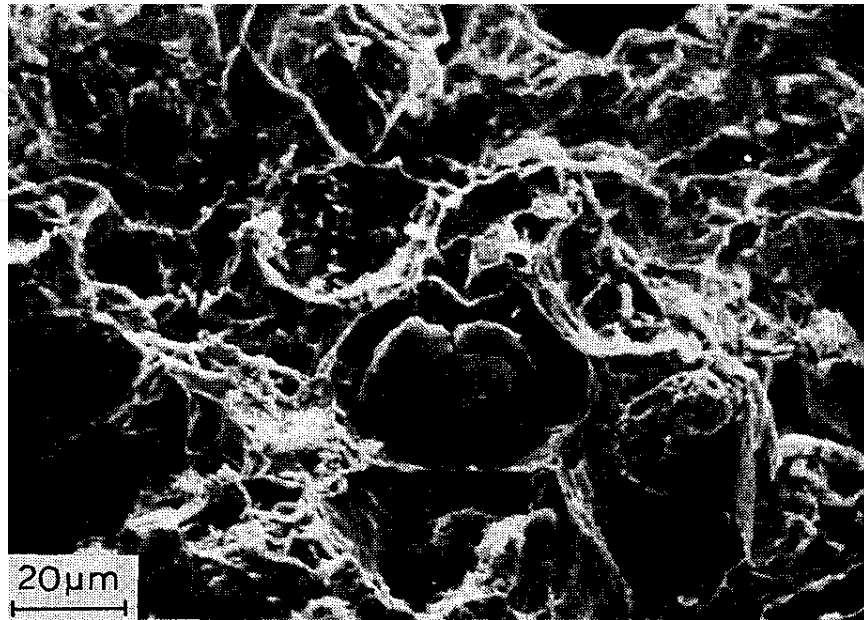


**Figure 13.** Fibrous fracture in the stable crack growth region of 2% Si casting Source: S. Seetharamu [10]



**Figure 14.** Transgranular cleavage in crack growth region of 3% Si casting Source: S. Seetharamu [10]



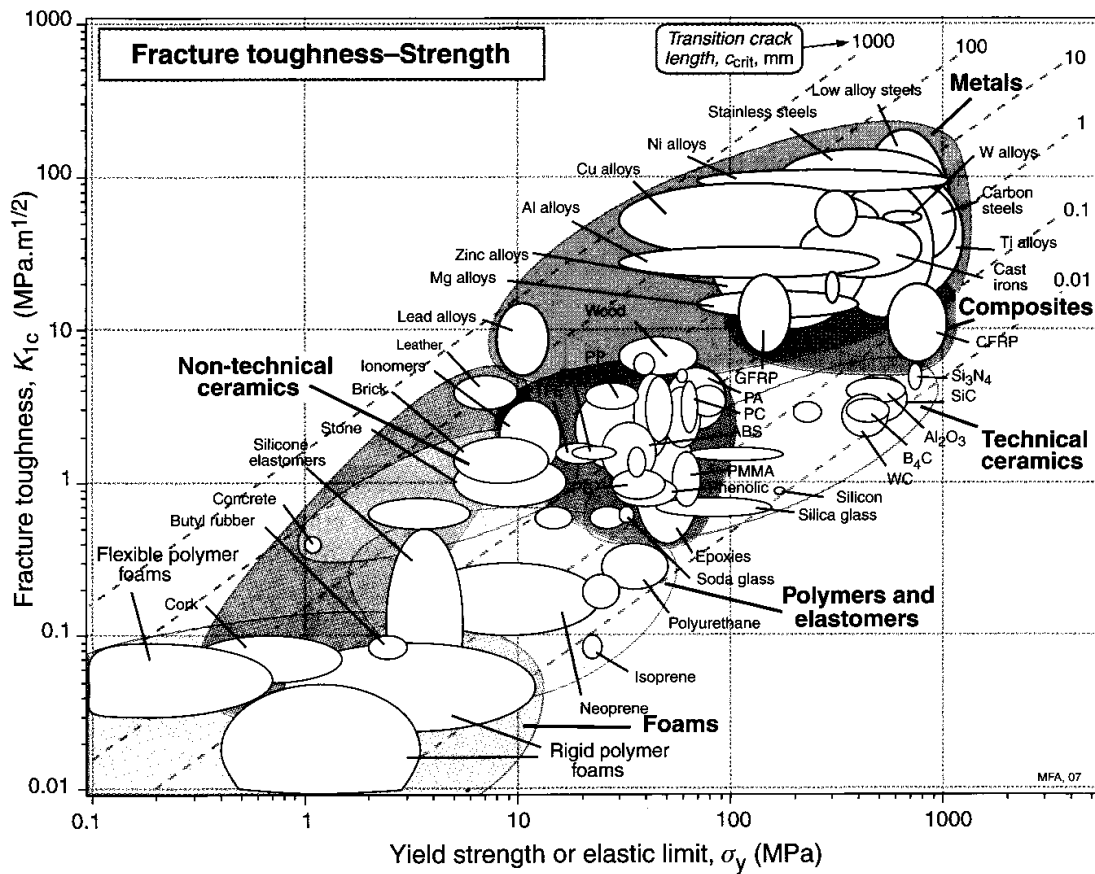


Figure 15. Fracture toughness, yield strength and transition crack length of materials. Source: M.F. Ashby, et al [5]

A relatively new development in the field of ductile irons is Austempered Ductile Iron (ADI) which is commercially available in different grades [40]. The fracture toughness of ADI can be in the range of about 59-86 MPam<sup>1/2</sup> and therefore exceeds the fracture toughness of most other ductile iron grades, except Ni-resist. The fracture toughness values are best determined using EPFM. However, Lee, et al [41] have used ASTM E399, which seems to be justified as the ratio 2.5 (K<sub>IC</sub>/σ<sub>ys</sub>)<sup>2</sup> is below the test sample thickness of 25 mm; as the authors have not reported the yield strength, but only the Brinell hardness, the yield strength (MPa) is assumed to be 3.3 times the Brinell hardness, for the purpose of making this statement..

It is important to realize that both stress and crack size should be within limits for safe use of any casting. When the failure mode is brittle, the critical flaw size is given by equation (1) when K<sub>I</sub> reaches a critical value K<sub>IC</sub>. When there is significant crack tip plasticity the transition from stable crack growth to unstable mode occurs at a length given by

$$C_{crit} = \left( \frac{K_{IC}}{\sigma_{ys}} \right)^2 \frac{1}{\sqrt{\pi}} \tag{17}$$

In Figure 15 is shown a plot of fracture toughness versus yield strength with the transition crack length (mm), based on equation 14, of different values shown as parallel broken lines. All materials cut by a given transition crack line will have the same transition crack length. It would be a great benefit to the casting industry if similar charts are available only for casting alloys.

## 5. Summary

This chapter first deals with the basics of fracture toughness testing and microstructure development in castings. Several publications on fracture toughness of aluminum alloys, steel and different types of cast iron have been reviewed with intent to note the typical values of fracture toughness and infer that the values are affected by not only the type of alloy but the processing adopted to make the castings. There is need to minimize extrinsic processing defects (for example, bifilms [28,42] in drossing alloys, shrinkage, porosity and others) so that the intrinsic fracture toughness, governed by the bond and dislocation mobility is approached, if highly fracture-resistant castings are to be produced. Of course this problem should be tackled based on cost-benefit relationship. The need for further research in this area is clearly evident.

## Acknowledgements

Dr. T.L. Anderson is sincerely thanked for permission to use the numerous illustrations and equations used in this chapter. The authors also acknowledge the permission to use illustrations from other distinguished book authors referenced in this chapter.

## Author details

M. Srinivasan<sup>1</sup> and S. Seetharamu<sup>2</sup>

<sup>1</sup> Department of Mechanical Engineering, Lamar University, Beaumont, Texas, USA

<sup>2</sup> Materials Technology Division, Central Power Research Institute, Bangalore, India

## References

- [1] Ashby, M. F., Shercliff, H., & Cebon, D. (2007). *Materials: engineering, science, processing and design*, Elsevier, Amsterdam, 167.

- [2] Hertzberg, R. W. (1983). *Deformation and Fracture of Engineering Materials*, John Wiley and Sons, New York, 353.
- [3] Hertzberg, R. W. (1983). *Deformation and Fracture of Engineering Materials*, , John Wiley and Sons, New York, 355.
- [4] Ashby, M. F., Shercliff, H., & Cebon, D. (2007). *Materials: engineering, science, processing and design*, Elsevier, Amsterdam, 164.
- [5] Ashby, M. F., Shercliff, H., & Cebon, D. (2007). *Materials: engineering, science, processing and design*, Elsevier, Amsterdam, 173.
- [6] Schey, J. A. (2000). *Introduction to Manufacturing Processes*, McGraw-Hill, Boston, 209.
- [7] (2012). [http://www.termwiki.com/EN:linear\\_elastic\\_fracture\\_mechanics](http://www.termwiki.com/EN:linear_elastic_fracture_mechanics).
- [8] (2012). <http://www.public.iastate.edu/~gkstarns/ME417/LEFM.pdf>.
- [9] Anderson, T. L. (2005). *Fracture Mechanics*, Taylor and Francis, Boca Raton, 300.
- [10] Seetharamu, S. (1982). *Ph.D. thesis*, Indian Institute of Science.
- [11] E399-97. (1997). *Standard Test Method for Plane Strain Fracture Toughness of Metallic Materials*, American Society for Testing and materials, Philadelphia, PA.
- [12] Anderson, T. L. (2005). *Fracture Mechanics* Taylor and Francis, Boca Raton , 310.
- [13] E1820-01,. (2001). *Standard Test Method for Measurement of Fracture of Toughness*, American Society for Testing and materials, Philadelphia, PA.
- [14] Anderson, T. L. (2005). *Fracture Mechanics*, Taylor and Francis, Boca Raton, 308.
- [15] Anderson, T. L. (2005). *Fracture Mechanics*, Taylor and Francis, Boca Raton, 321.
- [16] Anderson, T. L. (2005). *Fracture Mechanics*, Taylor and Francis, Boca Raton, 322.
- [17] Smith, W. F. (1981). *Structure and Properties of Engineering Alloys*, McGraw-Hill, Boston, 203.
- [18] Smith, W. F. (1981). *Structure and Properties of Engineering Alloys*, McGraw-Hill, Boston, 208.
- [19] Hafiz, M. F., & Kobayashi, T. (1996). Fracture toughness of eutectic Al-Si casting alloy with different microstructural features. *Journal of Materials Science*, 31, 6195 -6200.
- [20] Kumai, S., Tanaka, T., Zhu, H., & Sato, A. (2004). Tear toughness of permanent mold cast DC A 356 aluminum alloys. *Materials Transactions*, 45(5), 1706-1713.
- [21] Tirayakioglu, M. (2008). Fracture toughness potential of cast Al-7%Si-Mg alloys. *Materials Science and Engineering A.*, 497, 512-514.
- [22] Speidel, M. O. (1982). *6th European Non-Ferrous Industry Colloquium of the CAEF.*, 65-78.
- [23] Staley, J. T. (1976). Properties related to fracture toughness. *ASTM STP.*, 605, 71-96.

- [24] Tohgo, K., & Oka, M. (2004). Influence of coarsening treatment on fatigue strength and fracture toughness of Al-Si-Mg alloy castings. *Key Engineering Materials*, 261-263, 1263-1268.
- [25] Kwon, Y. N., Lee, K., & Lee, S. (2007). Fracture toughness and fracture mechanisms of cast A356 aluminum alloys, *Key Engineering Materials*, 345-346, 633-636.
- [26] Alexopoulos, N. D., & Tirayakioglu, M. (2009). Relationship between fracture toughness and tensile properties of A357 cast aluminum alloy. *Metallurgical and Materials Transactions*, 40A, 702.
- [27] Lee, K., Kwon, Y. N., & Lee, S. (2008). Effects of eutectic silicon particles on tensile properties and fracture toughness of A356 aluminum alloys fabricated by low-pressure casting, casting-forging and squeeze casting processes. *Journal of Alloys and Compounds*, 461, 532-541.
- [28] Tirayakioglu, M., & Campbell, J. (2009). Ductility, structural quality and fracture toughness of Al-Cu-Mg-Ag (A201) alloy castings. *Materials Science and Technology*, 25(6), 784-789.
- [29] (2012). *FRACTURE TOUGHNESS IN RELATION TO STEEL*, [www.sfsa.org/sfsa/pubs/misc/Fracture%20Toughness.pdf](http://www.sfsa.org/sfsa/pubs/misc/Fracture%20Toughness.pdf).
- [30] Barnhurst, R.J., & Gruzleski, J.E. (1985). Fracture toughness and its development in high purity cast carbon and low alloy steels. *Metallurgical Transactions A.*, 16A, 613-622.
- [31] Chen, L., Zhao, Y. X., & Song, G. X. (2011). Random critical fracture toughness values of China railway Grade B cast steel wheel. *Key Engineering Materials*, 480-481, 381-386.
- [32] Kim, C. K., Park, J. I., Lee, S., Kim, Y. C., Kim, N. J., & Yang, J. S. (2005). Effects of alloying elements on microstructure, hardness and fracture toughness of centrifugally cast high-speed steel rolls. *Metallurgical and Materials Transactions A.*, 36A, 87-97.
- [33] James, L.A., & Mills, W.J. (1988). Fatigue-crack propagation and fracture toughness behavior of cast stainless steels. *Engineering Fracture Mechanics*, 29(4), 423-434.
- [34] Elliott, R. (1983). *Eutectic solidification processing*, Butterworths, London, 194.
- [35] Walton, C.F., & Opar, T.J. (1981). *Iron castings handbook*, Iron Castings Society, 263.
- [36] Walton, C.F., & Opar, T.J. (1981). *Iron castings handbook*, Iron Castings Society, 357.
- [37] Salzbrenner, R. (1987). Fracture toughness behavior of ferritic ductile iron. *Journal of Materials Science*, 22, 2135-2147.
- [38] Doong, J., Hwang, J., & Chen, H. (1986). The influence of pearlite fraction on fracture toughness and fatigue crack growth in nodular cast iron. *Journal of Materials Science*, 21, 871-878.
- [39] Bradley, W.L., & Srinivasan, M.N. (1990). Fracture and fracture toughness of cast irons. *International Materials Reviews*, 35, 156.

[40] (2012). <http://www.ductile.org/didata/section4/4intro.htm#Austempering>.

[41] Lee, S., Hsu, C., Chang, C., & Feng, H. (1998). Influence of casting size and graphite nodule refinement on fracture toughness of austempered ductile iron. *Metallurgical and Materials Transactions A*, 29A, 2511-2521.

[42] Campbell, J. (2003). *Castings*, Elsevier.

IntechOpen

IntechOpen